

Nonstrictly-Ergodic Signals In Road Roughness Analyses: A Theoretical And Experimental Study

Praticò Filippo Giammaria

Associate Professor - DIMET Department - Mediterranean University of Reggio Calabria

Synopsis

The purpose of this paper is confined to the modelling and interpretation of road profiles.

As is well known, in roughness studies and researches it is possible to individualize a widespread scenario of modelling tools and survey technologies.

They all have, in different ways, the purpose of informing Road Engineers about the state and the evolution of pavement roughness: Rod and level survey, Dipstick profiler, Profilographs, Response type road roughness meters (RTRRMs), Profiling devices, for example.

Progressively, both in classification theory and analyses, Fourier decomposition and Transforms, dynamic systems theory and averaged parameters were used, to furnish reliable information related to sections of a certain length L , sometimes implicitly considered as a part adequately similar to the entire process.

This means analyzing a process with behavioural attributes which are quite comprehensible by means of observation of the road profile, which is, in any event to be considered as a set of simply readable signals, that is to say, ergodic signals.

Unfortunately, road pavements seem not to be a simple confirmation of this underlying "signal organization"; in fact, road localized phenomena are intrinsically part of any actually existing (new or old) road. They lie in a dominion of interference between two main sets: roughness and distress, and can affect importantly comfort and safety levels.

In the light of these problems, a theoretical and experimental study was conducted.

Main road/airport localized roughness (AASHTO Standard Practice PP 51-03, Fernando and Bertrand 2002 methodology) were previously identified and properly classified and a specific experimental investigation was designed and performed in order to collect other information useful in classifying localized roughness.

Following the classification and interpretation, some important algorithms concerning longitudinal road profile transforms (IRI, etc.) were implemented.

After this phase, in order also to detect phenomena which are not strictly speaking ergodic, some models and signal transforms (not involving Fourier Transforms, averaged indicators or stationarity hypotheses) were proposed and accurately tested on experimental data versus traditional analysis methods (Power Spectra, Power Spectral Density, IRI, etc.).

In the light of the obtained results and interpretations, by referring to the established targets, it is possible to highlight that IRI philosophy of roughness, being conceived for simulating effective human discomfort, is cumulative and averaged; so it can't be very useful for "local-global" analyses.

On the other hand, the Fernando and Bertrand technique is simple and very effective, but it focalizes only half of the problem here studied; the other half is explained by the classical Fourier analysis (P_{zz} spectra).

Continuous wavelet algorithms seem to fit sufficiently the targets of weighing up and pondering both the event localization and the spectral interpretation. Some limitations in localized roughness localization and interpretation can anyhow arise in particular conditions and so partially sidestep the double appraisal.

More research is needed in order to dispose of a greater variety of samples, by analysing more surface defects and formalizing a definitive procedure for the identification of the type of distress; more reliability, transportability and generalization will be so achieved.

Nonstrictly-Ergodic Signals In Road Roughness Analyses: A Theoretical And Experimental Study

PROBLEM STATEMENT

Automotive wheel tracks define two skew-lines in \mathfrak{R}^3 (i.e., if one refers them to a time-space sequence, two signals in time and space). These lines belong to pavement surface and transportation efficiency depends largely on its surface and mechanic properties.

In particular, road surface state (given that the pavement is just the tire interface) has a primary importance and it influences safety, comfort, transportation costs, etc.

So, the evaluation of the pavement surface becomes more and more significant in the context of pavement management systems.

In particular, by evaluating the state of pavement surface, it is possible to:

- optimize pavement design, materials, construction techniques;
- quantify pavement condition and performance;
- dispose of reliable support in maintenance and rehabilitation decisions, by establishing maintenance priorities;
- predict pavement performance (Cebon, 2000).

In evaluating pavement conditions, there is a problem, whose nature is both theoretical (Signal Processing Theory) and technological (hardware and software): surface state is “handled” by a conceptual bifurcation into two main categories: roughness and distress.

Roughness can be defined as a distortion of the pavement surface that contributes to an undesirable or uncomfortable ride (Hudson, 1978).

On the other hand, some distresses can contribute to an uncomfortable ride and may be detected by roughness measurements of the class 1 (FHWA, 2003).

Importantly there isn't always a clear gap between these sets and some surface, non-recurrent phenomena, if correctly detected, can be analysed both as localized roughness and as particular distresses (e.g. depressions, pushing, showing, bumps, potholes).

The above-cited non-recurrence of some phenomena is below identified and analysed by the signal theory and by the concepts of stationary and ergodic signals.

Leaving aside empirical solutions (e.g. PSI), the main consequences of this “logical split” are many doubts in survey planning, interpretation and value-assessing (axiology, epistemology) and a certain “scientific disease” in dealing with the same problem (surface defects) with a “double”, “asymmetric” approach.

In the light of the above-mentioned problems and uncertainties, the goal of this paper is confined to the analysis, formalisation and validation of algorithms for road signal processing, able to operate in that interference dominion between roughness and distress.

The paper is organized into three parts: 1) analysis of the state-of-the-art (by referring to roughness and distresses, §2); 2) problem modelling (§3); 3) experimental validation (§4).

PHENOMENA AND MEASUREMENTS

This paragraph deals with roughness and distress phenomena and measurements. Survey technologies, criteria and indicators are collected, analysed and logically organized in order to dispose of a sound and reliable state-of-the-art position before approaching problem modelling in the next paragraph.

Survey Technologies

Distress evaluation is often a complex and 3D operation. It can be performed visually (by not-automated measurements) or by surface video images, at highway speed, by particular vans equipped with high-resolution cameras. After automated surveying, it is possible to perform a manual evaluation (team of individuals, experts) or an automated evaluation using computer software. Main phases are: video-recording, in-van real time return, automatic evaluation. The most important advantages are efficiency, quality control, precision, safety in collecting data, availability to other data processing.

Roughness evaluation is usually a 2D operation and it can be performed by the techniques in figure 1. This organization summarizes a considerable amount of examined devices, reported in table 5 in the appendices.

Integrated analysis units can evaluate: a) longitudinal and transverse profile and pavement texture; b) distress and pavement video; c) grade (longitudinal) and slope (transverse); d) GPS coordinates; e) panoramic right-of-way video and feature location.

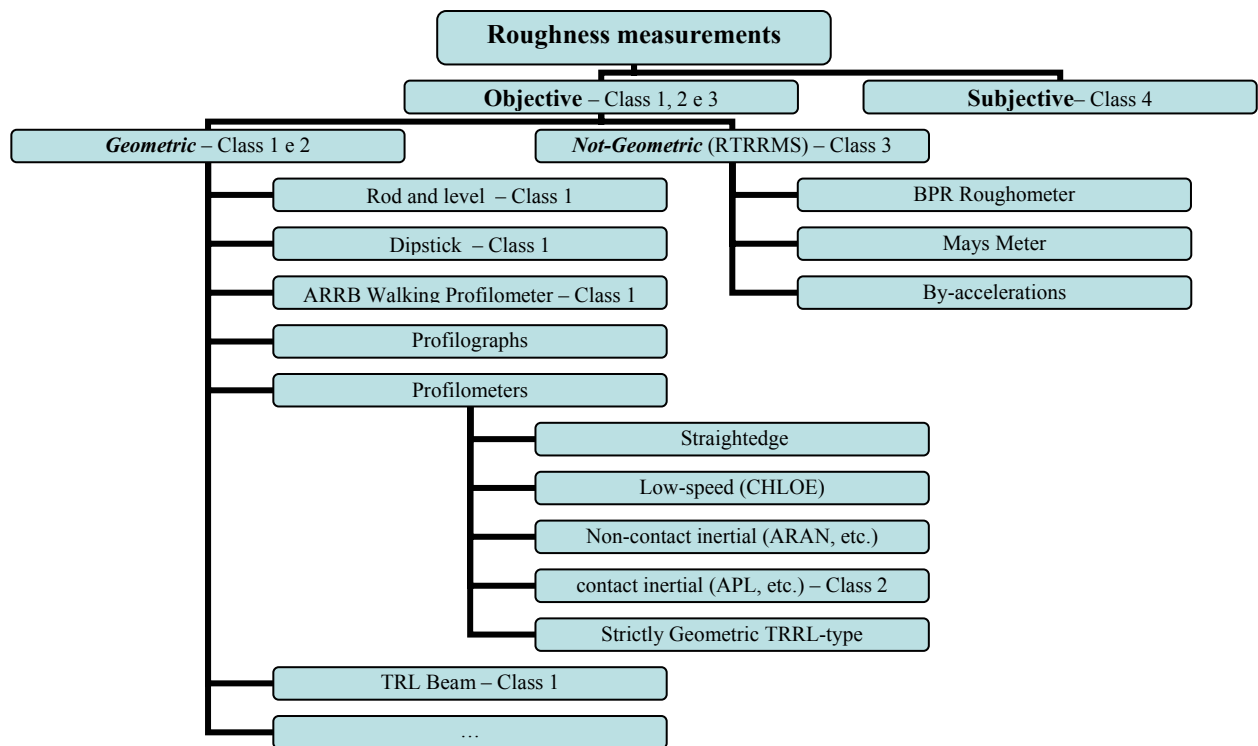


Figure 1 – Roughness: main techniques, devices and classes

Codifying and classifying Criteria For Surface Analyses

Logical criteria in pavement surface evaluation can be categorised as follows:

- a) spatial frequency content, with an implicit hypothesis of signal stationarity and ergodicity (these terms will be better explained as follows; in practice they mean: “as matter-of-fact I can survey this wheel track, today, from here to there, and I can understand at once all the stochastic process”). So it is possible to distinguish micro, macro, mega, unevenness (scientific literature in this field is quite considerable (CNR, 1988; Boscaino and Praticò, 2001; Boscaino and Praticò, 2002; Boscaino, Praticò, Vaiana, 2003);
- b) characteristic dimensions (single chip surface, etc.);
- c) cause;
- d) effects (in service availability, in mechanics, etc.); it is possible to individualise five categories: cracking, patching and potholes, surface deformation, surface defects, others-miscellaneous distresses (FHWA, 2003);
- e) distress mechanics (fracture, distortion, disintegration).

A summary of the major flexible pavement distresses, with a short dimensional description, is reported in table 6, in the appendices. On the basis of this analysis one can appreciate that the distresses number 1, 2, 4a, 7, 9, 11, 15, 16, 17, 18 can't in general be properly detected by non-contact high-speed devices, owing to the minimum allowable step (about 10-15 cm).

An outline of the most important indicators used in surface description is reported in the following table 7, while the main correlations among surface indicators are reported in table 8. It is important to put emphasis on the fact that all these correlations are referred to conventionally stationary and most-of-all ergodic, road signals (see, in particular, the last ones). Among the indicators, the IRI and the Power Spectra may be often considered as worthy of note in roughness studies (see table 7, indicators n.44, 9; table 8, n.1; table 9, n.1), while an interesting strategy for detecting localized roughness (better described below) seems to be that suggested by Fernando and Bertrand (Fernando and Bertrand, 2002, see table 7 n.45).

As is well known, in a given point of a pavement, roughness is time-dependent. This fact may constitute another plain experience of not-stationarity (for a fixed point of the surface) and can be an interesting topic for not-ergodic or/and non-stationary studies. An inventory of models concerning roughness time-dependence is reported in table 9.

PROBLEM MODELLING

This paragraph deals with actual road signal anomalies (that is to say roughness and distresses) in terms of signal theory. Road signal is analysed and a specific algorithm is proposed and prototypically tested.

Fundamentals For A Possible Theory of Pavement Surface Defects

In Signal analysis, one way to study and codify different signals is the phenomenological one (see figure 2). By this methodology signals can be categorized as deterministic, random, (not-) stationary, (not-) ergodic.

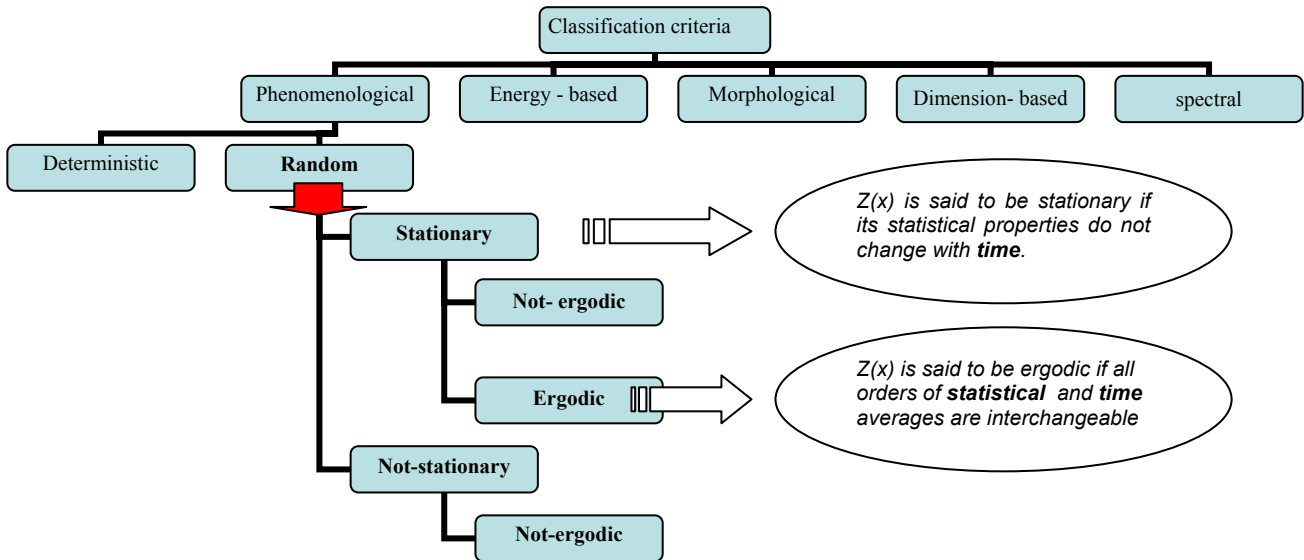


Figure 2 Classification criteria

As is well known, actual signals are often random.

Let $Z(x, \rho) \equiv Z(x)$ be a continuous random process, x the time or space, ρ_i (e.g. ρ_1, ρ_2, \dots) the various samples. For a fixed x , $Z(x)$ is a random variable (see figure 3). For a fixed ρ , $Z(x)$ is a non-random function of x .

For fixed ρ and x , $Z(x)$ is a real number (e.g. 5 mm). If z is one of the values of $Z(x)$ and $f(z; x)$ is the first-order density function, $\eta(x) = E[Z(x)]$ is the expected value of $Z(x)$.

Then it is

$$\eta(x) = E[Z(x)] = \int_{-\infty}^{\infty} z \cdot f(z; x) \cdot dz \quad (1)$$

$Z(x)$ is said to be stationary if its statistical properties do not change with time (see figure 3). For example, when $x=x_1$, it is:

$$\eta(x) = E[Z(x)] = \int_{-\infty}^{\infty} z \cdot f(z) \cdot dz \quad (2)$$

and the same result may be obtained for $x=x_2$.

In a wide sense (Wide-Sense Stationarity, WSS), a process $Z(x)$ is said to be stationary if the above-mentioned mean is constant (i.e. time-invariant) and the autocorrelation

$$R(\tau) = E[z(x)z(x + \tau)] \quad (3)$$

depends only on the time (or space) difference and not on two time variables x and $x+\tau$.

In practice (especially when there are a few samples), the sample is split into many parts (slices), by searching the stationarity for each of them. In this operation it can be useful to estimate, for the single subset, mean square values (i.e. $R(0) = E[z(x)z(x)]$), in order to detect non-random trends, for example, by counting reverse arrangements (that is to say inversions) and by comparing them with probabilistic predictions.

In order that the theory of stochastic processes be practically useful, it is necessary that the observations of a stochastic process may be used to evaluate, for example, the average. With regard to this topic, $Z(x)$ is said to be ergodic if all orders of statistical and time averages are interchangeable. In this case, if one

considers all the samples at only one time $x=x$, it is $\eta(x) = \int_{-\infty}^{\infty} z \cdot f(z) \cdot dz$; on the other hand, if one considers only one sample at all the times it is

$$\eta(x) = \lim_{T \rightarrow \infty} \frac{1}{2T} \int_{-T}^T Z(x) dx, \quad (4)$$

where x is defined in T . For an ergodic process, both (2) and (4) give the same result.

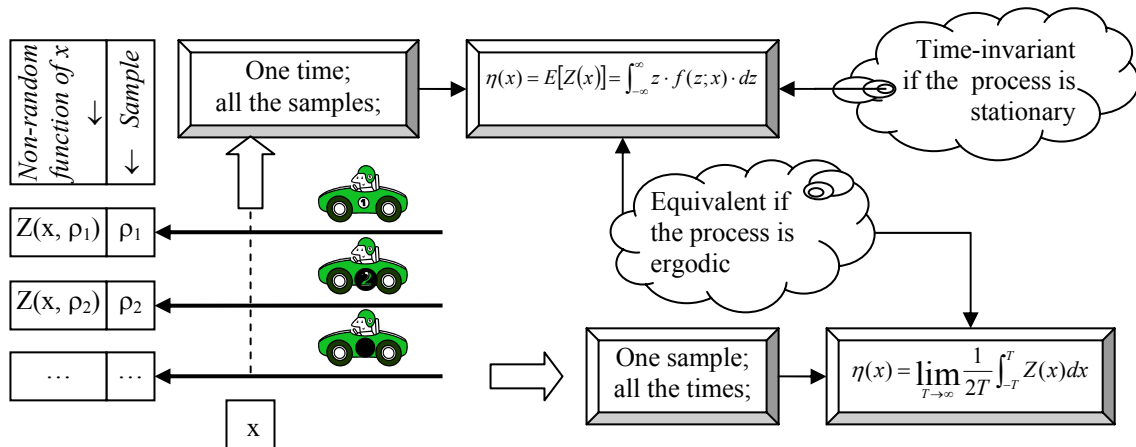


Figure 3 Stationary and Ergodic processes

It is extremely interesting that, generally speaking, an ergodic process is always stationary too. In fact, an average determined “along” a single sample is (in theory) calculated in $-\infty, +\infty$, and so it is time-invariant. So all the averages are, for any sample and for the ensemble, time-invariant, that is to say the process is stationary. On the contrary, a stochastic process doesn’t need to be strictly stationary in order for it to obey to an ergodic theorem (Parzen, 1999).

In practice, after a set of profiles has been surveyed (for example, right and left wheel track and centre), specific programs give profiles plots, IRI plots and values. Another method, very useful in mechanistic approaches, consists in determining Power Spectra (P_{zz}) or Power Spectrum Densities (PSDs), by Fourier analysis. More recently, Fernando and Bertrand (Fernando and Bertrand, 2002) codified an interesting technique to detect “localized roughness”, based on the deviations of the profile $P_0(x)$ from the moving average $P_f(x)$, determined by the well-known technique of the moving average (base=7.62m). In this process, a suitable threshold for bump detection and potential must-grind locations was identified in 3.5mm~4mm. The method can be summarized as follows: “If, for x , $|\Delta(x)| = |P_0(x) - P_f(x)| \geq \varepsilon$, then x identifies a localized roughness” (e.g., bump, with $\varepsilon=3.8\text{mm}$, and $P_0(x) - P_f(x) > 0$).

In principle, it is possible to observe that both usual approaches (profiles and IRI plots, spectral algorithms) and Fernando and Bertrand method seem to present some specific characteristics:

- profile plots are very difficult to interpret both in terms of roughness and distresses; moreover they are often filtered, in order to satisfy IRI algorithm, and then they are asymmetric and present manifest distortions; so, especially for the thickness of the localized roughness, they can only give a small amount of information;
- IRI plots and values provide information “averaged” and “cumulative” (that’s IRI philosophy) and it results quite impossible to combine both roughness and distress analyses;
- Power Spectral Density and power spectrum are the result of a Fourier analysis and then they are both theoretically and practically influenced by the effective ergodicity (and, obviously, stationarity) of the signal; in this way, a not-ergodic signal introduces an anomaly in $\log f_s - \log P_{zz}$ spectrum, but this fault is probably analysed by the wrong algorithm;
- The Fernando and Bertrand method seems to possess the power of simplicity and efficiency; nevertheless, it is a technique for detecting (only) localized roughness, not a criterion for analysing simultaneously both ergodic and not-ergodic road signals.

The proposed model (amplifying of the dimensions of transforms space)

The underlying idea of the proposed model is here explained. All the above-mentioned criteria (P_{zz} , IRI, Fernando and Bertrand) are profile-based applications and “move” from the profile to a function defined in \mathfrak{R}^1 . In this space (or range) one can distinguish two conditions: a) profile is quite elapsed. The new variable is a frequency, then, implicitly, there is a stationarity and ergodicity hypothesis, with a practical independence from the initial point; b) the new variable is similar to the profile abscissa. So, it is very difficult to understand stationary components. In view of this, it may be interesting to amplify the dimensions of the space, using Short Fourier Transforms or wavelet transforms (Walker, 1999). According to the problem of multi-resolution, here *continuous* wavelet algorithms are considered, with the following assumptions:

1. Let the time parameter be here called t and referred to the single point surveyed by the profiler;
2. Let the scale parameter be here called s and referred (by a dimensional coefficient) to the wavelength.

The Morlet-Grossmann definition of the continuous wavelet transform for a 1D signal $F(x) \in L^2(\mathfrak{R})$ is:

$$W(s,t) = \frac{1}{\sqrt{s}} \int_{-\infty}^{+\infty} F(x) \psi^* \left(\frac{x-t}{s} \right) dx \quad (5)$$

where z^* denotes the complex conjugate of z , $\psi^*(x)$ is the analyzing (“mother”) wavelet, $s(>0)$ is the scale parameter and t is the position parameter. The transform is characterized by the following three properties:

1. it is a linear transformation,

$$2. \text{ it is covariant under translations: } F(x) \longrightarrow F(x-u) \quad W(s,t) \longrightarrow W(s,t-u) \quad (6)$$

$$3. \text{ it is covariant under dilations: } F(x) \longrightarrow F(\xi x) \quad W(s,t) \longrightarrow s^{-0.5} W(\xi s, \xi t) \quad (7)$$

For the last property, the wavelet transform can be very effective in analyzing hierarchical structures and may be considered like a mathematical microscope with properties that do not depend on the magnification. If a function $W(s,t)$ is the wavelet transform of a given function $F(x)$, it can be shown that $F(x)$ can be

$$\text{restored using the formula: } F(x) = \int_0^{+\infty} \int_{-\infty}^{+\infty} \frac{1}{\sqrt{s}} W(s,t) \psi \left(\frac{x-t}{s} \right) ds dt \quad (8)$$

There are many wavelet classes. In the following table some of the major ones are summarized.

class	1. Crude wavelets.	2. Infinitely regular wavelets.	3. Orthogonal and compactly supported wavelets	4. Biorthogonal and compactly supported wavelet pairs.
Examples	gaussian wavelets, morlet, mexican hat.	meyer.	Daubechies (dbN, see below the figures 8 to 11, in which the db10 is used), symlets, coiflets.	B-splines biorthogonal wavelets
Main properties	- phi does not exist. - the analysis is not orthogonal. - psi is not compactly supported. - the reconstruction property is not insured. Possible analysis: - continuous decomposition. Main pleasant properties: symmetry, psi has explicit expression.	- phi exists and the analysis is orthogonal. - psi and phi are indefinitely derivable. - psi and phi are not compactly supported. Possible analysis: - continuous transform. - discrete transform but with non FIR filters. Main particular properties: symmetry, infinite regularity. Possible analysis: - continuous transform. - discrete transform.	- phi exists and the analysis is orthogonal. - psi and phi are compactly supported. - psi has a given number of vanishing moments. Potential: - continuous transform. - discrete transform using FWT. Good properties: support, vanishing moments, FIR filters. Specific properties: For dbN : asymmetry For symN : near symmetry For coifN: near symmetry and phi as psi, has also vanishing moments.	- phi functions exist and the analysis is biorthogonal. - psi and phi both for decomposition and reconstruction are compactly supported. - phi and psi for decomposition have vanishing moments. - psi and phi for reconstruction have known regularity. Potential: - continuous and discrete transform (using FWT). Good properties: symmetry with FIR filters, desirable properties for decomposition and reconstruction are split and nice allocation is possible.
Dif-ficulties	fast algorithm and reconstruction unavailable.	fast algorithm unavailable.	poor regularity.	orthogonality is lost.

In practice, in the light of the above-mentioned, for a profile analysis, the continuous wavelet transform $W(s, t)$, herein called $cwt(s, t)$, gives a surface on the axes s (which is the scale parameter and takes into account space frequencies) and t (which takes into account the profile abscissa).

The plots of $cwt(s, t)$ may show some peaks (herein called $\max cwt$); these peaks have given values of scale (herein called S_{opt}) and given values of t (identifying the ratio x/ρ , where x is the abscissa of the profile and ρ is the sampling step).

On the basis of the formula (5), cwt consists of a collection of discrete correlations of the signal (i.e. profile), with discrete samplings of the functions (Walker, 1999)

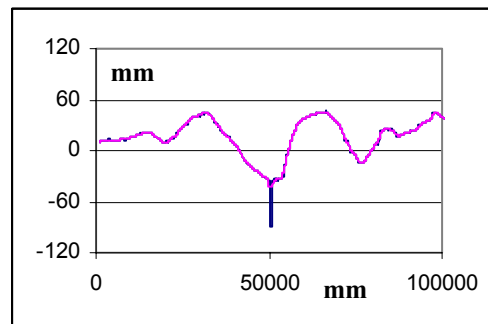
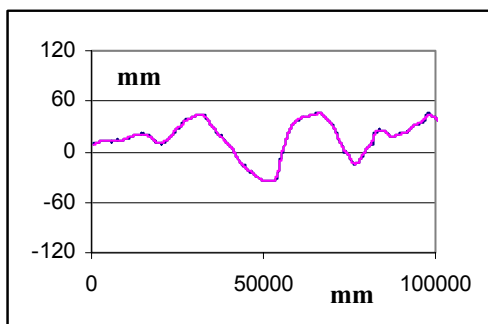
$$\frac{1}{\sqrt{s}} \psi \left(\frac{x}{s} \right), \quad s > 0 \quad (6)$$

For this, being the function ψ like a small wave or peak, a point in which there is a $\max cwt$ can represent a good correlation between the profile and a given peak, i.e. an irregularity.

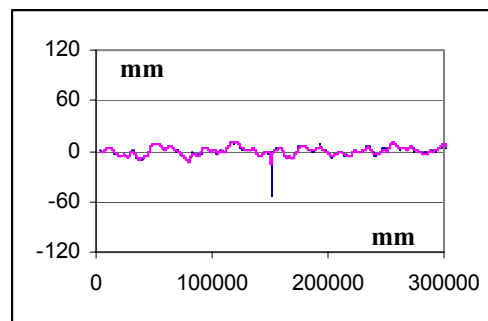
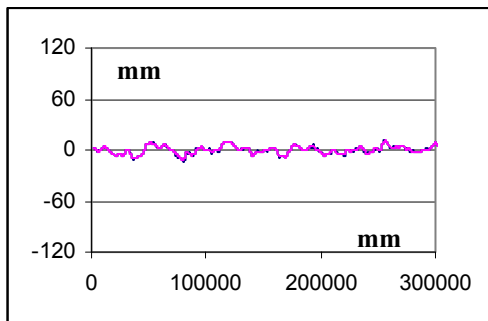
SIMULATIONS, EXPERIMENTS AND INFERENCES

In order to evaluate the capability of wavelets to individualize both not-ergodic and stationary-ergodic components, a specific research plan, both theoretical and experimental, was designed. Table 2 resumes both the main phases of the experiments and the characteristics of the profiles here analyzed and reported in figures 4 to 7.

Table2 Research plan	
Phases	
1-st phase	Basic (spatial) properties inference on ideal profiles
2-nd phase	Survey and phenomenological analysis of profiles and distress
3-rd phase	Statistical analysis (precision)
4-th phase	Not-strictly ergodic signals analysis by IRI, classical Fourier analysis, Fernando and Bertrand method, wavelet transforms
Survey Area localization	Calabria (Italy)
Profilometer class	Class I, ASTM E950
N.o of Surveyed profiles	124= (4wheel tracks)*(31 repetitions)
Profiles characteristics	1: Step=102mm; L=102m; 1*: As profile "1"but with one pothole 50mm deep and 600mm long; 2: Step=305mm; L=305m; 2*: As profile "2"but with a pothole 50mm deep and 600 mm Long



Figures 4 and 5 Surveyed profiles number 1(left) and 1*(right)



Figures 6 and 7 Surveyed profiles number 2(left) and 2*(right)

Before applying the algorithm to a true road signal, many tests were effected on ideal signals (sinusoids), with or without defects (bumps, potholes, etc.), by varying wavelength λ (mm), amplitude A (mm), sampling step (for example 100~300 mm), defect geometry (mean depth H , mm, and length L , mm). By referring to the plots $cwt(s, t)$, the major results are here summarized:

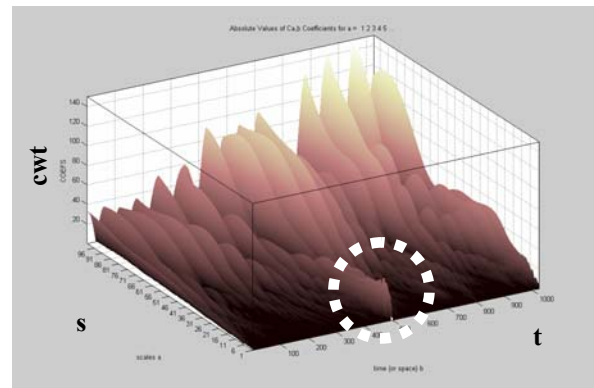
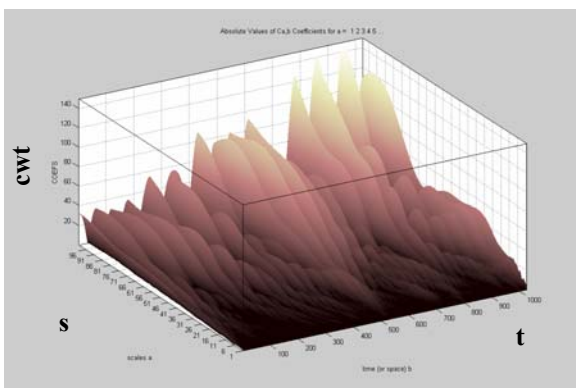
- for stationary-ergodic components, $S_{opt}=(\lambda/\rho)\cdot\beta_1$, where S_{opt} stands for the value of scale which optimizes cwt , λ is the wavelength, ρ is the sampling step, β_1 is a real number;
- for stationary-ergodic components, $\max cwt=(\lambda/\rho)^\alpha\cdot A\cdot\beta$, where $\max cwt$ stands for the maximum value of the continuous wavelet transform, λ is the wavelength, ρ is the sampling step, A is signal amplitude, α and β are real numbers;
- for non stationary-ergodic components, $S_{opt}=(L/\rho)\cdot\beta_2$, where S_{opt} stands for the value of scale which optimizes cwt , L is the defect length, ρ is the sampling step, β_2 is a real number;
- for non stationary-ergodic components, $cwt(S_{opt})=(L/\rho)^{\alpha_1}\cdot H\cdot\beta_3$, where H stands for the high of the defect;
- just the presence of an optimum in t -axis may be expressive of a non-ergodic occurrence, of a distress;
- the length of the scale axis influences cwt values;
- not-stationary, not-ergodic events correspond to remarkable peaks with double curvature;
- stationary signals correspond to single curvature cwt -surfaces (i.e. such as a ridge-line);

- some limitations and problems must be solved, regarding the localization of anomalies with characteristic dimensions similar to the wavelengths of stationary components, especially for small heights.

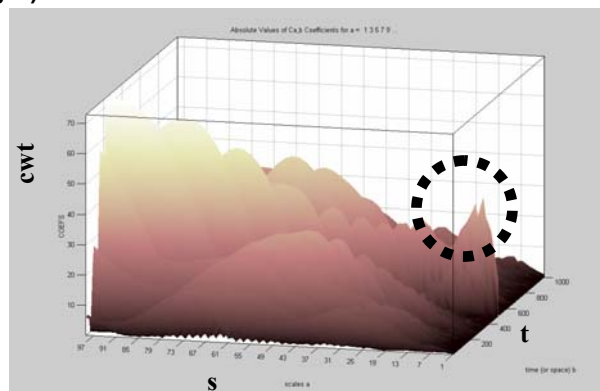
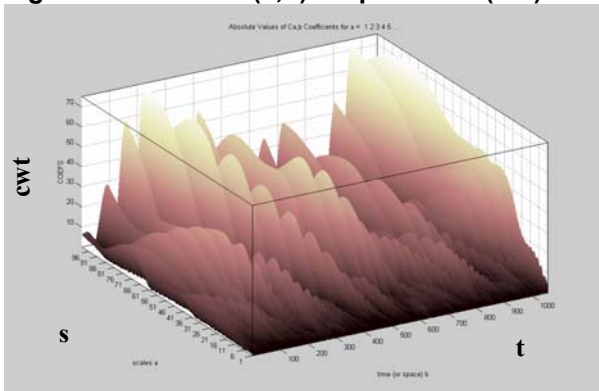
After the 2-nd phase (Survey and phenomenological analysis of profiles and distress) and the 3-rd phase (Statistical analysis - precision), among the 124 surveyed profiles (by an inertial profiler), four profiles (one for each wheel track, called 1, 1*, 2, 2*) were then processed by seven different wavelets classes (Mexican hat, Morl, db45, db10, db1, shan 115, bior1), so obtaining 28 different cwt 3D plots. In the figures from 8 to 11 only db10 applications are reported; dotted lines remark localized roughness. Figure 8 refers to profile 1 (see figure 4), while figure 9 refers to profile 1* (cfr. figure 5).

By comparing figure 8 with figure 9, one can observe that for a certain value of t (that is to say for a given abscissa $x=\rho t$) and for a certain value of s (which can give information about the length of the irregularity) the $cwt(s, t)$ of the profile 1* (right) presents an evident peak (dotted circle). It corresponds to the localized phenomenon which occurs for an abscissa equal to about 50000mm and this information is given by a plot (figure 9) which contains also spectral information.

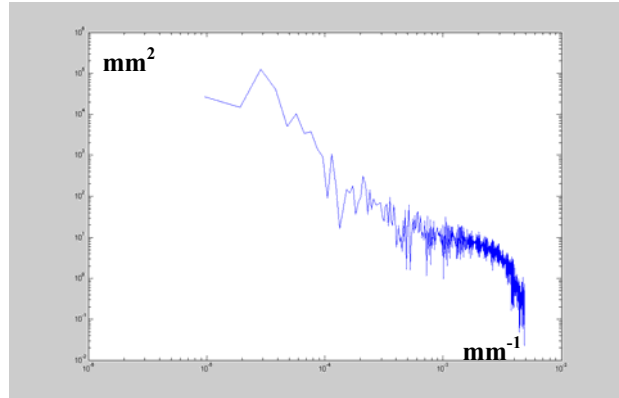
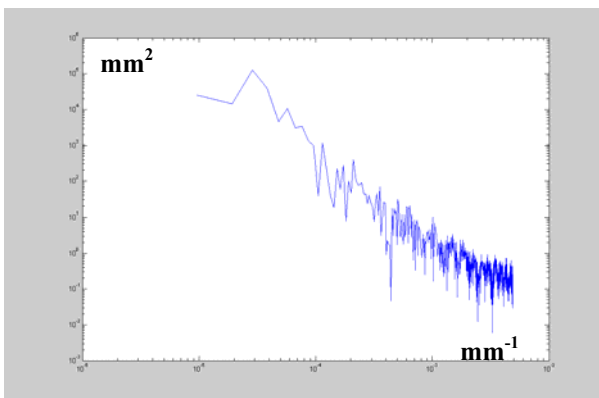
The above cited four profiles were also processed by IRI steady-state algorithm (so obtaining four different IRI plots), by FFT (Fast Fourier Transforms, so obtaining four Power Spectra, see figures from 12 to 15), and by Fernando and Bertrand method (see figures from 16 to 19).



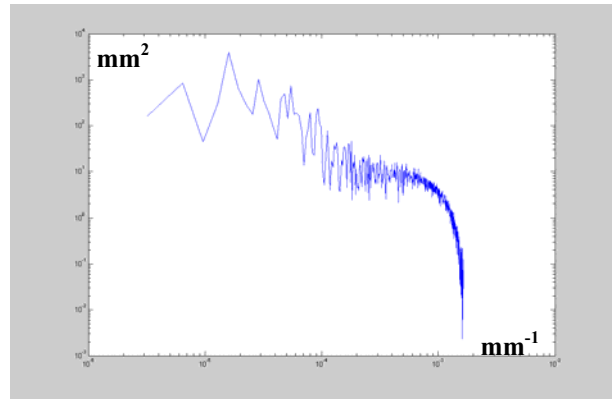
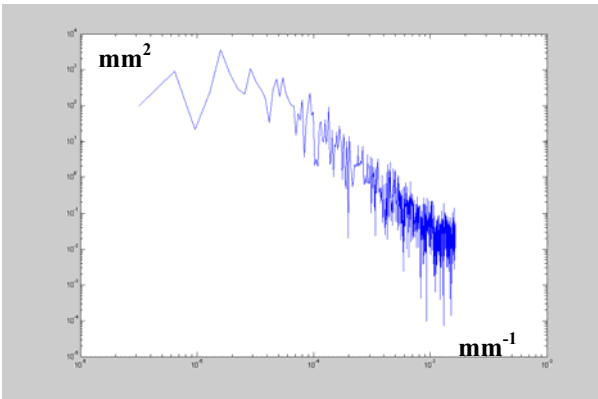
Figures 8 and 9 $cwt(s, t)$ for profiles 1 (left) and 1*(right)



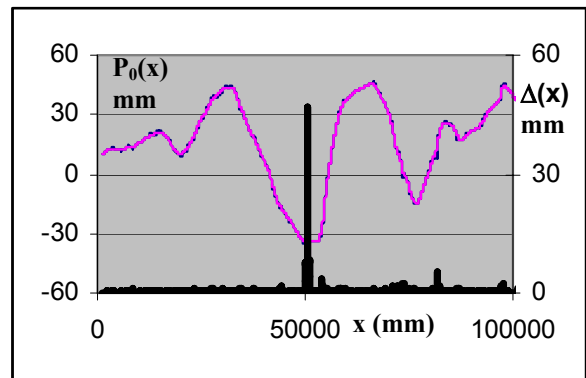
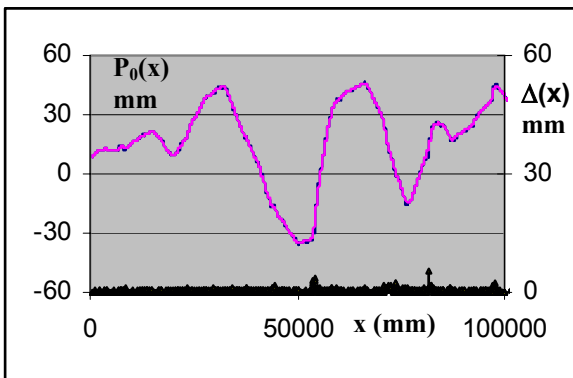
Figures 10 and 11 $cwt(s, t)$ for profiles 2 (left) and 2*(right)



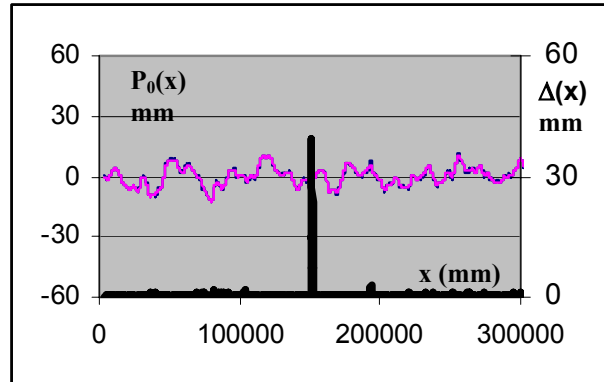
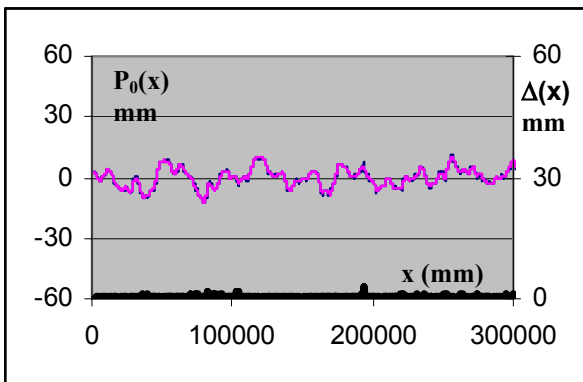
Figures 12 and 13 $P_{zz}(f_s)$ for profiles 1 (left) and 1*(right)



Figures 14 and 15 $P_{zz}(f_s)$ for profiles 2 (left) and 2*(right)



Figures 16 and 17 $P_0(x)$ and $\Delta(x)$ for profiles 1 (left) and 1*(right)



Figures 18 and 19 $P_0(x)$ and $\Delta(x)$ for profiles 2 (left) and 2*(right)

Results can be interpreted as follows. By referring, for example, to the difference between profiles 1 and 1* one can observe that wavelets coefficients seem able to detect both stationary and not-stationary components (see figures from 8 to 11).

If one compares the information content of power spectra and wavelets coefficients plots it is possible to put in evidence that while anomalies are well identified (both in wavelength and time or space occurrence) by wavelets, defects affect power spectra in different terms. In 1* and 2* profiles (that is to say the profiles with defects) P_{zz} (mm^2) decreasing behavior is certainly modified (compare, for example, figures 14 and 15) but both the spatial-frequency content and the time-space occurrence of the anomaly seem quite difficult to detect.

On the contrary, P_{zz} main suggestion consists in quantitative information about signal amplitudes (Boscaino and Praticò, 2001). If one interpolates P_{zz} plots in terms of log-log behavior, it is possible to highlight that star-profiles (e.g. profiles with not-ergodic components) have different P_{zz} range and different grade (see table 3).

Table 3 Fitting Power Spectra P _{zz} (f _s) log-log curves						
Profile	P_{zz} range (mm²)	f_s range (mm⁻¹) →	2·10 ⁻⁵ ~2·10 ⁻⁴	2·10 ⁻⁴ ~3·10 ⁻³	3·10 ⁻³ ~5·10 ⁻³	
1	10 ⁻³ ~10 ⁶	Equation→	-2.6·log ₁₀ f _s -8.0			
1*	10 ⁻² ~10 ⁶	Equation →	-2.3·log ₁₀ f _s -6.5	-1.2·log ₁₀ f _s -2.4	-7.2·log ₁₀ f _s -17.6	
Profile	P_{zz} range (mm²)	f_s range (mm⁻¹) →	2·10 ⁻⁵ ~2·10 ⁻⁴	2·10 ⁻⁴ ~10 ⁻³	10 ⁻³ ~2·10 ⁻³	X
2	10 ⁻⁵ ~10 ⁴	Equation→	-2.4·log ₁₀ f _s -8.6			
2*	10 ⁻³ ~10 ⁴	Equation →	-1.8·log ₁₀ f _s -5.6	-0.6·log ₁₀ f _s -1.1	-18.2·log ₁₀ f _s -54.0	
Note: f _s =1/λ: spatial frequency (mm ⁻¹); P _{zz} : signal power spectrum (mm ²);						

It is noteworthy that while the power spectrum of the profile 1 ranges from 10⁻³ to 10⁶, the power spectrum of 1* ranges between 10⁻² and 10⁶ mm², with a very sloping curve for high frequencies (log₁₀P_{zz}=-7.2·log₁₀f_s-17.6).

This difference may be due to the pothole, whose dimension (along the wheel track) is about 600mm (600¹≅2·10⁻³mm⁻¹).

In the same way, for profile 2*, power spectrum is contained in a smaller P_{zz} range than for the profile called 2.

In short, these differences (stationary versus stationary+not-ergodic) in power spectra may be summarized as follows:

1. different mean grade and not uniform grade;
2. different P_{zz} range.

Unfortunately, the information about localized roughness position is here elapsd.

If one considers the IRI ratio (ΔIRI%(1, 1*)=100·[IRI(1*)- IRI(1)] ·[maxIRI]⁻¹, see table 4), the influence of the pothole seems quite evident (36%), but, importantly, in a practical survey, the problem is what could be the causes.

Table 4 IRI and Δ(x)				
↓Profile ↓	↓IRI(mm/m) ↓	↓ΔIRI% ↓	Δ(x) (mm)	Δ Δ(x)%
1	2.15·K ₁	36%	1	98%
1*	3.37·K ₁		48	
2	5.21·K ₂	13%	1	98%
2*	5.96·K ₂		40	
Note: K ₁ , K ₂ : constants; (ΔIRI%=100·[IRI(i*)- IRI(i)] ·[maxIRI] ⁻¹); Δ(x)= P ₀ (x)-P _f (x) ; ΔΔ(x)%= (Δ(x) _i - Δ(x) _i)/ maxΔ(x)				

The fact that ΔIRI%(2, 2*), in comparing 2 and 2*, has a lower value than ΔIRI%(1, 1*), in comparing 1 and 1*, 13% versus 36%, may be due to the higher ratio between stationary and defect component power for the profiles 2 and 2*.

In considering such non-strictly ergodic signals, the quasi-continuity meaning is significant and noteworthy, both in s- and in t-scales: it introduces a remarkable drawback in all the stationary-based correlations, including that in (Wei and Fwa, 2004, see table 8, correlations number 13, 14, 15), which are very interesting but are based on few discrete wavelet transforms energy indices. Moreover, it seems quite manifest that time-space localization can constitute a clear advantage in processing non-strictly ergodic signals.

By referring to the Fernando and Bertrand algorithm, the Δ-function (there implicitly defined as Δ= | P₀(x)-P_f(x) |)

seems to be very effective in detecting a large part of localized phenomena (see figures 17 and 19 and table 4). In table 4, both Δx and the corresponding gradients are summarized.

Finally, some problems and some interesting features can be put in evidence about these specific wavelet applications:

1. Owing to the fact that S_{opt}≅(λ/ρ)·β₁, for a given S_{opt}, the value of λ can be easily determined (λ≅ρ·S_{opt}·β₁⁻¹) and so compared with the frequency f_s of the power spectrum (f_s=λ⁻¹≅ρ⁻¹·S_{opt}⁻¹·β₁); this feedback may be useful also in a synergic use;
2. for a given f_s (and then λ=f_s⁻¹), while the P_{zz} values are conditioned by statistics (then are higher if that component is present in all the signal), cwt values depend especially on the energy of the event (even though it's "alone" in a stationary and ergodic "sea");
3. the previous point explains the reason for which, in an effective profile, P_{zz} is (often) an essentially decreasing function, while the same profile has a not-monotone cwt(s) plot;
4. more research is needed in order to formalize a detailed procedure for distress identification;
5. some limitations and problems must be solved, regarding the localization of anomalies when the characteristic dimensions are similar to stationary components wavelengths, especially for small heights;

6. as is well known, some irregularities can compromise both comfort and safety; the problem is ruled (see figure 20) by irregularity dimensions (horizontal and vertical), vehicle speed, vehicle mechanics, with a certain difference between heavy vehicles and cars. It is very interesting that, as above inferred, max cwt depends both on L/ρ and H and both safety and comfort may depend on these factors. The corresponding relations may be monotonic respect H but not respect L/ρ (to be compared with footprint for resonance conditions). These facts could create a certain interest for max cwt in safety or comfort issue. However, the proposed method may be useful in pavement management, which constitutes a support for optimizing systematically both safety and comfort.

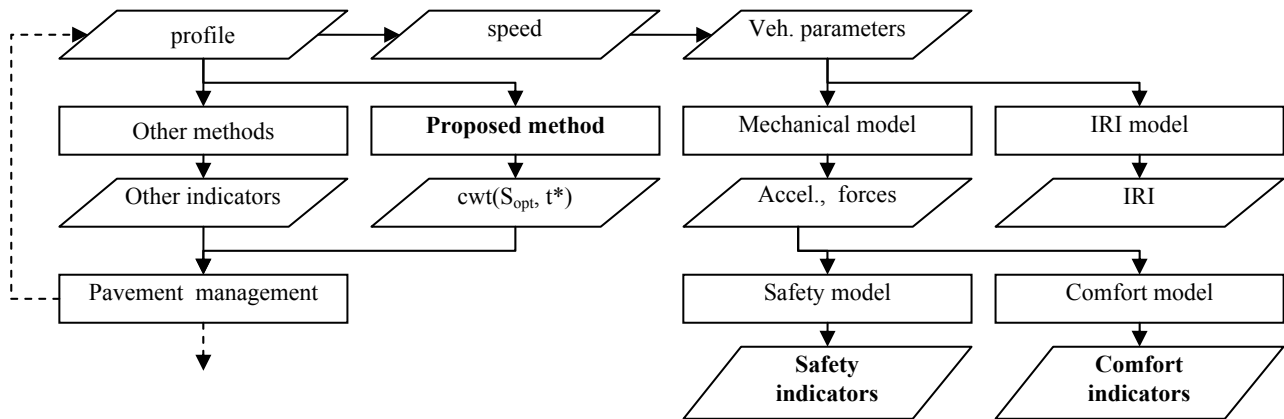


Figure 20 Relationship between the proposed method and safety/comfort problems

CONCLUSIONS

In the light of the obtained results and interpretations, by referring to the established targets, it is possible to highlight that IRI philosophy of roughness, being conceived for simulating the effective human discomfort, is cumulative and averaged, so it can't be very useful for "local-global" analyses.

On the other hand, the Fernando and Bertrand technique is simple and very effective, but it focalizes only half of the problem here studied; the other half is explained by the classical Fourier analysis (P_{zz} spectra).

Continuous wavelet algorithms seem to match sufficiently the targets of weighing up and pondering both the event localization and the spectral interpretation.

Corresponding quantitative parameters, such as the three coordinates scale-translation-cwt that identify localized roughness, are very informative and may be very useful in pavement management and so for optimizing safety and comfort.

Some limitations in localized roughness localization and interpretation can anyhow arise in particular conditions and they can partially sidestep the double appraisal local-global.

More research is needed in order to dispose of a great variety of samples, by analysing more surface defects, so giving more reliability, transportability and generality to these sentences.

Other efforts may be useful in formalising accurate procedures for distinguishing the various types of distress or localized roughness.

REFERENCES

- AIPCR COMITTE, (1995), *Inventaire des appareils de mesure des caracteristiques de surface des chaussees*, AIPCR Association Internationale Permanente des Congres de la Route, Parigi, all the pages.
- Boscaino G., Praticò F. G., (2001), *Classification et inventaire des indicateurs de la texture superficielle des revêtements des chaussées*, B.L.P.C. n° 234- sept-oct 2001, France, pages 1 to 4.
- Boscaino G., Praticò F. G., (2002), *La tessitura e i requisiti funzionali delle pavimentazioni stradali*, Atti Convegno Infravia 2000, Verona.
- Boscaino G., Praticò F. G., Vaiana R., (2003), Spectral texture indicators significance in relation to flexible pavements surface performance, XXII PIARC World Road Congress, oct. 2003, Durban - South Africa, pages 1 to 5.
- Cebon D.,(2000), *Handbook of Vehicle-Road Interaction* – Swets & Zeitlinger Publishers, pag.115.
- Choubane B., Mcnamara R.L., (2001), Research Report State of Florida: *Precision of high-speed profilers for measurement of asphalt pavement smoothness*, FDOT – Florida Department of Transportation, pages 2 to 10.
- Consiglio Nazionale delle Ricerche, (1988), BU CNR n.125/88, *Istruzioni sulla pianificazione della manutenzione stradale*, Anno XXII, n.125, pages 1 to 15.

- Delanne Y., Pereira P., (2000), *Analyse de la relation entre l'uni et la qualité d'usage des routes – Application à la fixation de spécifications pour les travaux neufs et à la définition de classes d'uni pour la gestion de l'entretien*, Bulletin 228, LCPC 2000, pages 2 and 3.
- FEHRL, Forum of European National Highway Research laboratories, (2001), *Inventory of High speed longitudinal and Transverse road evenness measurement equipment in Europe*, technical Note 1999/01, pages 3 to 21.
- Fernando E., Bertrand C., (2002), *Application of profile data to detect localized roughness*, Transportation Research Board 81st Annual Meeting, January 13-17, 2002, Washington, D.C., USA, pag.1.
- FHWA, (2003), *Distress identification manual for the long term pavement performance program*, Publication no. FHWA-RD-03-031, June 2003, USA, pages 1 to30 and annex C.
- Huang Y.H., (2003), *Pavement Analysis and Design*, Pearson Prentice Hall, pages 368 to 401.
- Hudson et al., (1985), *Root-Mean Square Vertical Acceleration as a summary Roughness index*, ASTM Special Publication No.884, T.D. Gillespie and M. Sayers editors, Philadelphia, Pa, all the pages.
- Hudson W.R., (1978), generalised Roughness index, Annual meeting of the transportation RESERCH Board, Wasington, D.C., January.
- La Torre F., Ballerini L., (2002), *Valutazione dell'influenza della irregolarità longitudinale sul comfort dell'utente per la viabilità urbana – IX Convegno Internazionale*, Parma, 30-31, pages 1 to10.
- Parzen E., (1999), *Stochastic Processes*, Society for Industrial and Applied Mathematics, Philadelphia, pages 73 and 74.
- Patrick J., Bailey R., (2003), Use of Pavement Deterioration Models in Pavement Design, Opus International Consultants New Zealand, pages 1 to 10.
- Sayers M.W., Gillespie T.D., Paterson W.D.O., (1986), *Guidelines for conducting and calibrating road roughness measurements*, World Bank Technical Paper Number 46.
- Sayers M.W., Gillespie T.D., Queiroz C.V., (1986), *The International Road Roughness Experiment (establishing correlation and a calibration standard for measurements)*, World Bank Technical Paper Number 45.
- Smith K.L., Smith K.D., Evans L.D., Hoerner T.E., Darter M.I., (1997), *Smoothness Specifications for pavements – Final Report*, - National Cooperative Highway Research Program Transportation Board.
- Tammirinne N. et al.Editors, (2002), *Road Structures Research Program*, 94 -2001, Helsinki 2002, Finnish Road Administration [<http://www.tieh.fi/tppt/pdf/rep3702.pdf>], pages18 to 28.
- Walker J.S., (1999), *A primer on wavelets and their scientific applications*, Chapman &Hall/CRR, pages 7 to 11 of the chapter 4.
- Wei L. and Fwa T.F., (2004), *Characterizing road roughness by wavelet transform*, TRB2004 Annual Meeting, pages 1, 2, 5, 7, 8.

APPENDICES

	Device	Principle/Indicators/Producers/Users References
1.	Straightedge	Actual variation in road profile http://www.ndsu.nodak.edu/ndsu/ugpti/MPC_Pubs/html/MPC02-130.html
2.	Rolling Straightedge	Actual variation in road profile
3.	BPR Roughmeter	Response type
4.	Mays meter	*Response type – Rainhart Co., TX
5.	Rainhart Profilograph	Multi wheel profilograph Rainhart Co., TX http://www.ndsu.nodak.edu/ndsu/ugpti/MPC_Pubs/html/MPC02-130.html
6.	ARAN 4100, 4300, 4900 e PURD	Housing mounted – IRI (mm/m), RCI – Roadware Group Inc. Sineco, Autostrade SpA, /Rodeco/CRS (AIPCR, 1995), http://www.state.me.us/mdot/planning/pavement/aran.htm http://www.ndsu.nodak.edu/ndsu/ugpti/MPC_Pubs/html/MPC02-130.html www.roadware.com/customers.htm
7.	PURD	RCI – PSI – SDI – Rut depth – etc - University of Waterloo – Department of Civil Engineering – CANADA N2L 3G1 (AIPCR, 1995)
8.	CHLOE	Low speed
9.	GMR profilometer	Z(x)
10.	APL (Analyseur de Profil en Long)	Z(x) – LABORATOIRE CENTRAL DES PONTS ET CHAUSSEES (L.C.P.C.) – M.BOULET (AIPCR, 1995)
11.	California Profilograph APL	Multi wheel profilograph – California
12.	Rod and level	z(x) – low speed
13.	TRRL Abay beam	z(x)
14.	MERLIN	(Machine for Evaluation Rough. Using Low-cost Instrumentation) – Vertical displacement – Transport Research Laboratory – ENGLAND http://www.romdas.com/technical/tec-ciri.htm , (AIPCR, 1995)

15.	Dipstick profilometer	z(x) – IRI – FACE CONSTRUCTION TECHNOLOGIES, INC. 427 USA http://www.cedex.es/cec/documenti/survey.htm (AIPCR, 1995)
16.	TRRL High speed profilometer	z(x) – IRI – High speed
17.	ROSAN	IRI, Ride Number (RN) – ASTM E 950 & E 1926 – SURFAN ENGINEERING AND SOFTWARE, INC. – US http://www.tfrc.gov/focus/oct01/rosan.htm ; <a href="http://www.webs1.uidaho.edu/bayomy/IAC/42<sup>nd</sup>/Presentations_2002/ROSAN%20for%20Lynn.pdf">http://www.webs1.uidaho.edu/bayomy/IAC/42nd/Presentations_2002/ROSAN%20for%20Lynn.pdf ; http://www.tfrc.gov/pubrds/ianpr/rosan.htm
18.	'MGPSgeometry' and 'MGPSsurface'	pavement smoothness, roughness and texture properties portable, vehicle independent – MGPS – USA (-Surfan) – MGPS, Inc. – Texas Transportation Institute www.mgps-solutions.com/
19.	FHWA PSM	Non-contact sensors – Earthech, Inc., Baltimore, MD http://www.ndsu.nodak.edu/ndsu/ugpti/MPC_Pubs/html/MPC02-130.html
20.	ROMDAS 7000	Roughness – IRI - Bump Integrator – Data Collection Ltd. NEW ZEALAND http://www.romdas.com/surveys/sur-rgh.htm
21.	RST Laser	IRI – OPQ Systems – Sweden (AIPCR, 1995)
22.	Swedish laser RST	Accelerometer multipurpose - Novak, Dempsey & assoc., USA
23.	Video Laser RST II	OPQ Systems - Sweden
24.	Laser Portable RST PT 2	IRI – RMS – VTI, Sweden - OPQ SYSTEMS AB SWEDEN - (FEHRL, 2001) - (AIPCR, 1995)
25.	DYNATEST Road Surface Profiler 5051 MARK II	IRI – RN – Etc – Dynatest International A/S – Denmark http://www.dynatest.com/hardware/rsp.htm http://www.dynatest.com/addresses1/ordices.htm
26.	Dynatest 5000-RDM	IRI - etc – DYNATEST – Denmark (AIPCR, 1995)
27.	Computerized PROFIOGRAPH	NO IRI – ELE International – USA - http://www.soiltest.com/
28.	PAVESET Model ES2000 Profilograph – Paveset Road Design System – Paveset Grade Control	NO IRI – USA – Australia http://www.paveset.com/index.htm
29.	ARRB Walking Profiler	IRI – etc – Roadware Group Inc. – Canada http://www.roadauthority.com/database/Product.asp?prod=3460
30.	ARRB Profilometer	IRI – etc – Australian Road Research Board (AIPCR, 1995)
31.	ROADMASTER	IRI-Tester with GPS option http://www.al-engineering.fi/index.html
32.	Laser-profilograph	Laser based Profilometer for Road Surface Texture and Profile Measurements- AL-ENGINEERING OY – Finland http://www.al-engineering.fi/laser.html
33.	AL-ROADLAB	IRI – ROADMASTER device + others – AL-ENGINEERING OY - Finland http://www.al-engineering.fi/roadlab.html
34.	Axon1	IRI – RMS – etc – Oberon Data och Elektronik AB - Sweden http://www.oberon.se/axon1.htm
35.	SSI Standard Profilograph	NO IRI – Surface System e Instruments, LLC-USA - http://www.smoothroad.com/products/profilograph/
36.	High Speed Profiler System	IRI –simulated Profilograph Index (PI), ASTM Ride Number, etc. Surface System e Instruments, LLC – USA http://www.smoothroad.com/products/highspeed/highspeed.pdf ; SSI-profile.com
37.	Lightweight Profiler SSI	Surface System e Instruments, LLC – USA http://www.smoothroad.com/products/lightweight/
38.	Lightweight Profilers	IRI – RN – PI – INTERNATIONAL CYBERNETICS CORPORATION - http://www.internationalcybernetics.com/ltprofile.htm
39.	Full Size Profiler	IRI – RN – PI – INTERNATIONAL CYBERNETICS CORPORATION - http://www.internationalcybernetics.com/fsprofile.htm
40.	Rolling Surface Profilers(Sur-Pro) –SP 1000- SP 1000 – MD	IRI – RN – PI – INTERNATIONAL CYBERNETICS CORPORATION – USA http://www.internationalcybernetics.com/rollprofile.htm
41.	Model 4000 Computerized Profilograph	NO IRI – Ames Engineering, Inc. – USA http://www.amesengineering.com/amesprof.htm
42.	Model 6000 Lightweight Inertial Surface Analyzer LISA	IRI – RN – PI – RQI – Ames Engineering, Inc. – USA http://www.amesengineering.com/ameslisa.htm
43.	Model 8000 HSP High Speed Profiler Kit	IRI – RN – PI – RQI – HRI – Ames Engineering, Inc. – USA http://www.amesengineering.com/ameshsp.htm
44.	Model 8000 SmoothPave RTP® (Real Time Profiler)	IRI – RN – PI – RQI – Ames Engineering, Inc. – USA http://www.amesengineering.com/ameswet.htm
45.	COMPUTERIZED PROFIOGRAPH Model CS 8200	NO IRI – California test method 526, FHWA test method T 504, ASTM E1274 computerized specification – James Cox & Sons, Inc – USA http://www.jamescoxandsons.com/
46.	Profilometer/PCA meter (PCA	Response type – James Cox & Sons, Inc – USA

	Road meter)	
47.	VTI laser profilometer	Road and Transport Research institute (Sweden) http://www.vti.se/ordic/1-01mapp/vti4.htm http://www.networksplus.net/rpug/2002/1-Establishing%20Reference.pdf www.vti.se/edefault.asp
48.	Road profiling Trans-Tek 600 ADT	NO IRI – Trans-Tek, Inc. – USA http://www.transtekinc.com/Application%20Articles/Road_Prof.pdf
49.	LMI 2500 Laser Sensors	LMI 3D Machine Vision LMI Technologies Inc. – Canada http://www.lmint.com/cfm/index.cfm?it=901&Id=39&Se=88&Sv=0
50.	SELCOM SLS 5000 SELCOM SLS 6000	LMI 3D Machine Vision http://www.lmint.com/cfm/index.cfm?it=901&Id=39&Se=88&Sv=0
51.	PathRunner van profiler	IRI – Pathway services inc. – USA http://www.pathwayservices.com/runner/runner.htm
52.	LVS LaserVISION system	IRI – GIE Technologies Inc. – CANADA http://www.gietech.com/
53.	Survey Vans	Roughness Index (IRI). Profile measurements are also used to estimate rut depth and faulting – International Cybernetics Corporation – USA http://www.pascousa.com/frames7.htm
54.	GSI GOMACO Smoothness Indicator	NO IRI – GOMACO Corporation – USA http://www.gomaco.com/Resources/gsi.html

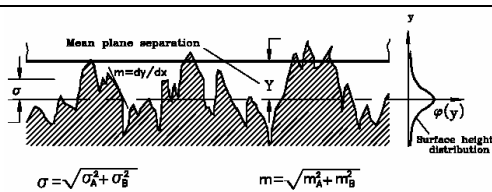
55.	Lightweight Profiler	IRI - PI – RN - International Cybernetics Corporation Engineering, Inc.- USA http://www.pascousa.com/frames7.htm
56.	GREENWOOD Profilograph	IRI – Greenwood Engineering A/S – Denmark http://www.greenwood.dk
57.	GREENWOOD LaserProf	IRI – Greenwood Engineering A/S – Denmark http://www.greenwood.dk/LaserProf/
58.	GREENWOOD MiniProf	Greenwood Engineering A/S – Denmark http://www.greenwood.dk/MiniProf/
59.	Class 1 + Laser Profilometer	IRI – Danish Road Research Institute- DANEMARK (AIPCR, 1995)
60.	Profiling Vehicle	IRI – etc – VTT Road and Traffic Laboratory – FINLAND (AIPCR, 1995)
61.	Road Rougness Meter	Road unevenness – Index Profile – NORVEGE (AIPCR, 1995)
62.	Road Surface Monitoring System ROADMAN	Road unevenness index, Longitudinal road profile – VTT Road and Traffic Laboratory – FINLAND (AIPCR, 1995)
63.	ALFRED	IRI – PUBLIC ROADS ADMINISTRATION – NORWAY (FEHRL, 2001); http://www.eapa.org/publications/1015.htm ; http://www.brcc.be/pdf/bul39.pdf
64.	ARGUS-KB	Schniering Ingenieurgesellschaft mBH – GERMANY (FEHRL, 2001)
65.	DYNVIA	SPRINC-DYNEX – CZECH REPUBLIC (FEHRL, 2001)
66.	FRMS Finnish Road Monitoring System	TECHNICAL RESEARCH CENTRE OF FINLAND (VTT) (FEHRL, 2001)
67.	HARRIS	GREENWOOD ENGINEERING ApS – DENMARK - (FEHRL, 2001)
68.	HRM High-Speed Road Monitor	IRI, - Longitudinal Road Profile – Transport Research Laboratory –WDM Ltd. – ENGLAND (FEHRL, 2001)
69.	KJLAW-T6500	IRI – SPAIN – USA (FEHRL, 2001)
70.	Model T6600	Inertial profilometer – USA
71.	K.J. Law 690 DNC	Rut depth – longitudinal profile – U.S.A. (AIPCR, 1995)
72.	K.J. Law 8300A	Roughness Index – U.S.A. (AIPCR, 1995)
73.	KP-514 MP « GAZEL »	NO IRI – Research and production centre « Rosdortech - RUSSIA (FEHRL, 2001)
74.	ORCA- Optical Road Condit Assess Vehicle	ORCA – Optical Road Condition Assessment Vehicle – ENGLAND (FEHRL, 2001)

75.	ZAG-VP	IRI – ZAG – VP – SLOVENIA (FEHRL, 2001)
76.	ROMEO	Transverse profile – FRANCE (FEHRL, 2001)
77.	TUS	Transverse profile - Rut depth – FRANCE – LCPC-Laboratoire central des Ponts et Chaussees Division Gestion de l'Entretien des Routes Centre de Nantes (FEHRL, 2001); (AIPCR, 1995)
78.	ULTRASONIC RUTMETER	Transverse profile –Rut depth – BELGIUM (FEHRL, 2001); (AIPCR, 1995)
79.	High Speed Survey Vehicle	Longitudinal road profile – Transport Research Laboratory ENGLAND (AIPCR, 1995)
80.	SIRST	Longitudinal profile - Federal Highway Administration – U.S.A. (AIPCR, 1995)
81.	South Dakota Profiling Device (South Dakota Road Profiler) KDOT South Dakota Type-Profiler	Profilometer principle - Plotted profiles and roughness ratings - South Dakota DOT - USA (AIPCR, 1995); http://www.pavement.com/PavTech/Tech/Dwnlds/TRB2003/03-2301.pdf
82.	Surface and Thickness Profilograph	Profile, - Surface course thickness - VTT Road and Traffic Laboratory - FINLAND (AIPCR, 1995)
83.	DQM2 Dynamisches Querprofil Messgerat	Cross profile - (AIPCR, 1995)
84.	Ornièromètre	Rut depth values - LCPC-Laboratoire central des Ponts et Chaussees Division Gestion de l'Entretien des Routes Centre de Nantes - France (AIPCR, 1995)
85.	PALAS Transverso-profilometre à Laser	Transverse profile - Video Image of Cross profile - LABORATOIRE CENTRAL DES PONTES ET CHAUSSEES (L.C.P.C-) - France (AIPCR, 1995); (FEHRL, 2001)
86.	QAG Querprofil Aufnahmegerat	Cross profile – ALLEMAGNE (AIPCR, 1995)
87.	Rutmeter	Transverse-profile - VTT Road and Traffic Laboratory - FINLAND (AIPCR, 1995)
88.	System zur Analyse der Quermebenheit	Cross profile, Rut depth, etc - ALLEMAGNE (AIPCR, 1995)
89.	PASCO Roadrecon	Accelerometer and laser sensor, Image file PASCO, Japan USA (AIPCR, 1995)
90.	PRO-RUT	FHWA, HNR-20 - U.S.A. - (AIPCR, 1995)
91.	SIRANO	LCPC-Laboratoire central des Ponts et Chaussees Division Gestion de l'Entretien des Routes Centre de Nantes - France (AIPCR, 1995)
92.	Bayerischer Unebenheitsmesser	Unebenheits index U160 (AIPCR, 1995)
93.	Bump Integrator	Road unevenness index - Danish Road Research Institute - DANEMARK (AIPCR, 1995)
94.	ROADMAN	IRI - AL-ENGINEERING OY - USA (AIPCR, 1995)
95.	WDM SCRIM ++	IRI - WDM Limited - ENGLAND http://www.wdm.co.uk/
96.	MRM-Multifunction Road Monitor	IRI - WDM Ltd – ENGLAND (FEHRL, 2001)
97.	MSHA ICC PROFILER	IRI http://www.ndsu.nodak.edu/ndsu/ugpti/MPC_Pubs/html/MPC02-130.html http://www.networksplus.net/rpug/2002/1-Laboratory%20Evaluation%20of%20Inertial%20Profiler%20Accuracy.pdf

Table 6 Flexible pavements main distresses

1. Aging surface
2. Alligator Cracking (m ² , SL)
3. Bleeding and Flushing – Excess Surface Asphalt (m ²)
4. Block cracking (m ² , SL) Surface: 0.1 0.1 m ² -9 m ² . One can individualize: 4a) Block cracking not-severe (< 12.7mm); 4b) Block cracking severe (> 12.7mm)
5. Pushing, corrugation and shoving, delamination (n, m ²)
6. Depression
7. Reflective Cracking (m)
8. Lane/shoulder drop-off or heave (mm)
9. Wheelpath Cracking, Longitudinal cracking, edge cracking (m, SL). One can individualize: not-severe (<

12.7mm length), and cracking severe (> 12.7mm length).
10. Patching (n, m ² , SL)
11. Polished aggregate (m ²)
12. Potholes – Chuck holes (n, m ² , SL)
13. Raveling (m ²)
14. Rutting (m ² , mm)
15. Slippage cracking
16. stripping – moisture damage
17. Thermal Cracking-Transversal Cracking (n, m, SL)
18. Water bleeding and pumping) (n, m ²)
19. Swell (m ²)
20. Joint damage (m)
Notes: n: number; m, m ² , mm: can be measured in m, m ² , mm; SL: there is a technique for assessing severity level

Table 7 Roughness indicators inventory	
Indicator [range] [measure units]	Expression References
1. International Roughness Index (IRI) [0 ÷ ∞]; [mm/m] [in/mile]	$IRI = \frac{1}{L_p} \cdot \int \left \dot{Z}_s - \dot{Z}_u \right dt; \quad IRI = \frac{\sum RS_i}{n-1}$ RS _i : rectified slope n: number of steps; PCC: $IRI = IRI_0 + C_1 CRK + C_2 SPALL + C_3 TF + C_4 SF; \quad IRI_R = IRI + \sigma_{IRI} Z_R$ (Sayers, Gillespie, Queiroz, 1986); (Sayers, Gillespie, Paterson, 1986); (Huang, 2003)
2. Half-car Roughness Index (HRI) [0 ÷ ∞]; [mm/m] [in/mile]	"When the IRI quarter-car analysis is applied to the averaged profile, the resulting index has been called the HRI". (Sayers, Gillespie, Queiroz, 1986); (Sayers, Gillespie, Paterson, 1986)
3. Mean Absolute Slope (MAS)	 <p style="text-align: center;"> $\sigma = \sqrt{\sigma_a^2 + \sigma_b^2}$ $m = \sqrt{m_a^2 + m_b^2}$ </p> <p style="text-align: center;"> http://www.mhtl.uwaterloo.ca/paperlib/papers/contact/general/gwnew.pdf </p>
4. Present Serviceability Rating (PSR) [0 ÷ 5]	Statistical parameter determined on the basis of panel rating www.cnsfarnell.co.uk/CNSF_English/roads.htm
5. Present Serviceability Index (PSI) ; [0-5]	$PSI = 5,03 - 1,91 \cdot \log_{10}(1 + SV) - 1,38 \cdot R_D^2 - 0,01 \cdot \sqrt{C + P}$ $PSI = 5,41 - 1,8 \cdot \log_{10}(1 + SV) - 0,09 \cdot (C + P)^{1/2}$ (HMA); (PCC)
6. Riding Comfort Index (RCI) ; [0 ÷ 10]	$RCI = a - b \cdot \log_{10} a_{eff}$
7. Power Spectral Density (PSD)	It is evaluated by Fourier transforms (see the references) (Smith et alia, 1997); (Boscaino and Praticò, 2002)
8. G(n0)	Power spectrum according to ISO 8608.
9. Power Spectrum (PS, P _{zz})	PSD not referred to the frequency range (Boscaino and Praticò, 2002)
10. L _T (λ)	Texture Level (10Log ₁₀ (a/a ₀) ²) (Boscaino and Praticò, 2002)
11. a _{mega}	indicator concerning megatexture amplitudes (Boscaino and Praticò, 2002)
12. Spectrum Analysis (DSQPS)	Spectral indicator measured by the French APL. http://perso.wanadoo.fr/r-et-l/APLUK.htm
13. PCA Roadmeter	response-type indicator, well correlated to MRN (below defined).
14. BPR Roughometer	response-type indicator, well correlated to MRN (below defined).
15. Average Rectified Slope (ARS)	It is a parameter determined by the profile, as SV.
16. Pavement Quality Index (PQI)	The Pavement Quality Index (PQI) provides a pavement condition rating
17. Surface Rating (SR)	The Surface Rating (SR) provides a pavement condition rating referred to surface state
18. RR	RR provide a measurement of rutting: $\log RR = -a + b \log(\omega_0) - c \log(N_{18}) + d \log(\sigma_c)$

	(Huang, 2003)
19. H_{APL}	It's determined by the French APL and depends on the spectral content of the profile. RMD (Rut Depth Mean, according to E1703- E1703M-95 ASTM) is a similar indicator (Boscaino and Praticò, 2002)
20. Pavement Condition Index (PCI) [0 ÷ 100]	PCI provides a pavement condition rating. www.piarc.lcpc.fr/pub/0105.i/trifr2-e.htm
21. Quarter Index (QI); [0 ÷ ∞]; [mm/m]; [in/mi]	$QI_r = -8,54 + 6,17 \cdot RMSVA_{1,0} + 19,38 \cdot RMSVA_{2,5}$, RMSVA is determined for a baseline of 1,0 m and 2,5 m (Smith et alia, 1997)
22. Ride Number (RN) [0 ÷ 5]	$RN_{Sayers} = 5 \cdot e^{-160 \cdot PI_{Sayers}}$; $RN_{Janoff} = -1,47 - 2,85 \cdot \log_{10}(PI_{Janoff})$ (Smith et alia, 1997)
23. Slope Variance (SV) [in/mile]	$SV = \frac{2B}{C^2} \cdot Var(\eta) \cdot E[R_D]^2$; B and C are referred to pavement properties; η is referred to variations; $E[R_D]$ is the rut depth averaged. $SV = \frac{\sum (S - \bar{S})^2}{n-1}$ (base=9 inches; step=1ft; S; single slope; N: number of samples; \bar{S} slope averaged. http://www.volpe.dot.gov/sbir/sol103/docs/vesvintro.doc ; (Huang, 2003)
24. Mays Ride Number (MRN) [in/mi]	MRN is obtained by cumulating vertical movements of a particular device and by referring the sum to the traveled distance. (Smith et alia, 1997)
25. Profile Index (PI); [0 ÷ ∞]; [mm/m]; [in/mi]	PI is a measure of profile deviations from an ideal plan http://www.odot.state.or.us/tddresearch/reports/smooth.pdf
26. Mays Meter Output (MO) [in/mi]	$MO = -20 + 23 \cdot C \cdot RMSVA_{4,2} + 58 \cdot C \cdot RMSVA_{4,9}$, where RMSVA is determined on a baseline of 1,2m and 4,9 m. (Smith et alia, 1997)
27. (NR)	Number of users that suggest a maintenance process: $NR = a - b$ (MPR) or $NR = a + b \log(PI)$, where a, b are coefficients, while MPR (Mean Panel Rating) and PI (Profile Index) are other indicators. (Huang, 2003)
28. NAASRA Roughness Measurement; (National Association of Australian States Road Authorities); [0 ÷ ∞]; [NAASRA]	It is determined by a standard mechanical device used extensively in Australia and New Zealand since the 1970s for measuring road roughness by recording the upward vertical movement of the rear axle of a standard station sedan relative to the vehicle's body as the vehicle travels at a standard speed along the road being tested. A cumulative upward vertical movement of 15.2 mm corresponds to one NAASRA Roughness Count (1 NRM/km). http://www.austroads.com.au/images/1/AM%20Glossary.pdf
29. CAPL₂₅ (EI)	It can be measured by APL (Analyseur de Profil en Long), v=6m/s, step= 25m. $EI = \frac{\sum_{i=1}^n u_i }{n}$ By the some APL device, it is possible to estimate NBO (Notes by wave band), IRI (International Roughness Index), DSQPS (Spectrum analysis), CP
30. NBO (Notation en bandes d'Onde) [1-10]	It can be measured by APL (Analyseur de Profil en Long); v= 20m/s; step= 5, 15 or 20cm, by three values, each of one referred to a different wavelength class: 0.7-2.8m; 2.8-11.2m; 11.2-44.8m (LPC n. 46/2000, DR 2000-36 -22.May 2000). $E_{BO} = 10^{-3} \cdot 50 \cdot \sum_{k=1}^{\frac{L}{\lambda_{BO}}} z_k^2$; $N_{BO} = a \ln E_{BO} + b$; $N_{PAN} = a + b N_{PO} + c N_{MO} + d N_{GO}$; $N_{PAN} = a + b \frac{N_{POd} + N_{POg}}{2} + c \frac{N_{MOd} + N_{MOg}}{2} + d \frac{N_{GOd} + N_{GOg}}{2}$ $N_{PAN} = a + b \frac{I_{IRId} + I_{IRIg}}{2}$; $N_{PAN} = -5.546 - 3.956 \ln(\gamma_{Is} + \gamma_{rs}) / 2$ (Boscaino and Praticò, 2002); (Delanne and Pereira, 2000)
31. SWE, MWE, LWE	Short, Medium and Long Wavelength Energy
32. Ride quality Index (RQI)	$RQI = 3 \ln(Var1) + 6 \ln(Var2) + 9 \ln(Var3)$. RQI can be determined by the PSD. Var1 - $\lambda=7.26$ m - 15.24 m (→base). Var2: $\lambda= 1.52$ m - 7.62 m. Var3: $\lambda= 0.61$ m - 1.52 m (→construction and compaction). High values mean great unevenness.
33. Mean Panel Rating (MPR)	Subjective, averaged indicator. The concept of Mean Panel Rating (MPR) evolved out of AASHTO road test in 1950s. It is the average of ratings given by a panel of pavement experts while driving over a given road stretch. After statistical processing, these ratings are processed to yield a single rating for the panel as a whole, which is called Mean Panel Rating (MPR). Thus, MPR gives an idea about the average degree of discomfort of riding over a given road stretch. Panel ratings depend strongly on the instructions given to the members of the panel to define what physical properties or quality is to be judged. Thus, MPR is a subjective judgment of road roughness. Development of MPR is based on psychophysical principles which must be carefully followed to obtain a valid panel ratings. http://www.ieindia.org/publish/cv/0503/may03cv6.pdf
34. Floor Flatness (FF) o (FN) and Levelness Numbers (FL)	Roughness indicator according to (ASTM-E 1155), usually applied to PCC. They may be determined by the Rolling Surface Profilers (SurPro).
35. Pavement Condition Rating (PCR)	It's a generic expression to indicate an indicator concerning a pavement evaluation

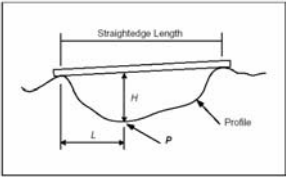
36. Band Pass Index (BPI)	<p>The Band Pass Index (BPI) was developed under National Cooperative Highway Research Program (NCHRP) funding. Like IRI, BPI is computed from a measured highway profile. First, the profile is filtered to remove wavelengths longer than 8 feet and shorter than 1 foot. Then the root mean square (RMS) of the filtered profile is computed to give the BPI. IRI and BPI are both average values derived from a filtered version of the highway profile. They differ in that 1) the IRI is accumulated axle movement and BPI is RMS, and 2) the IRI includes longer wavelengths. Note: The straightedge and bandpass filter indexes were initially considered as alternative to IRI. Once it was determined that IRI correlated best with driver perception, the straightedge and bandpass filter indexes were no longer required. http://www.fcny.org/cmgp/streets/pages/1998PDF/Report/6_TechApx.pdf</p>
37. Bump Index, 38. Bump Height, 39. Bump Length	<p>The Bump index (the shorter of the distance from the bump height position to the start of the straightedge and the distance from the end of the straightedge to the bump height position, H/H_R) concern localized roughness.</p>  <p>[http://www.fcny.org/cmgp/streets/pages/1998PDF/Report/6_TechApx.pdf]</p>
40. Structural Deduct (SD)	<p>The Structural Deduct (SD) is contained within the PCR, but indicates those distresses which may be related to the structural integrity of the pavement. A structural deduct of 25 or more indicates the pavement section should be considered for major rehabilitation. http://www.dot.state.oh.us/pavement/Pubs/PCR%20Forms.pdf; http://www.dot.state.oh.us/pavement/Pubs/Sect100.pdf; http://www.dot.state.oh.us/pavement/Pubs/PCR%20Forms.pdf</p>
41. AI	<p>Synthetic assessment for a road section: (AI=1 Good; AI=0 not-evaluable; AI=-1 bad) (La Torre and Ballerini, 2002)</p>
42. Mean Panel Rating Index; (IMPR)	<p>I_{MPR} is a subjective indicator. It is: $I_{MPR} = -\alpha - \frac{\beta}{\log I_{PSI}} \quad \text{and} \quad I_{MPR} = 5 \exp(-b I_{PI}^c)$ (Delanne and Pereira, 2000)</p>
43. Fernando and Bertrand index	<p>$\Delta(x) = P_0(x) - P_f(x)$ (Fernando and Bertrand, 2002)</p>
44. Root-mean-Square of VA, RMSVA	<p>RMSVA = $[\sum_i (L_{i+1} - L_i - L_i + L_{i-1})^2 \cdot D^{-2} \cdot (n-2)^{-1}]^{0.5}$, i=2, 3, ..., n-1. (Hudson et al., 1985); (Wei and Fwa, 2004)</p>
45. Mean Absolute of VA, MAVA	<p>MAVA = $\sum_i (L_{i+1} - L_i - L_i + L_{i-1}) \cdot D^{-3} \cdot (n-2)^{-1}$, i=2, 3, ..., n-1. (Hudson et al., 1985); (Wei and Fwa, 2004)</p>

Table 8 Correlations inventory

Indicator	Correlations References
1. International Roughness Index, IRI	<p>$IRI = 5,5 \cdot \ln\left(\frac{5}{PSI}\right)$; $IRI = 577,42 - 222,17 \cdot PSI + 25,664 \cdot PSI^2$ (R²=0,997); $IRI = 52,9 + 6 \cdot PI$ (R²=0,93); $IRI = 73,7 + 2,83 \cdot PI$ (R²=0,92); $IRI = 36,4 + 3,11 \cdot PI$ (R²=0,56); $IRI = 19,22 + 3,38 \cdot ARS - 0,0096 \cdot ARS^2$; $IRI = (QI_r + 10)/14$; $IRI = 31,552 + 1,7566 \cdot MO$ (R²=0,987); $IRI = 61,426 + 0,83577 \cdot MRN$ (R²=0,997); $IRI = 5,588 - 0,578 \cdot RCI$; $IRI = 563982,18 \exp(-1,51 RN)$; NASSRA = 28*IRI; IRI = (NAASRA + 1.27)/26.49; IRI=A+ΣB_iE_{di} (Smith et alia, 1997); (Sayers, Gillespie, Paterson, 1986); (Chourban et alia, 2001); (Patrick et alia, 2003); http://www.wsdot.wa.gov/ppsc/research/TRBSpecial/TRB2003-000311.pdf; (Wei and Fwa, 2004)</p>
2. Present Serviceability Rating, PSR	<p>$PSR = 5 \cdot e^{-0,18 \cdot IRI}$; $PSR = 5 \cdot e^{-0,26 \cdot IRI}$; $PSR = 5 \cdot e^{-0,24 \cdot IRI}$ (rural roads, highways, urban roads, L_{base}=320m); $PSR = 5 \cdot (1 + 0,7005935 \cdot (IRI_{50Km/h})^2)^{-0,204325}$ (urban roads, L_{base}=50m c.a., IRI[50Km/h]); $PSR = 5,697 - 2,104 \cdot \sqrt{IRI}$ (HMA); $PSR = 6,634 - 2,813 \cdot \sqrt{IRI}$ (PCC); $PSR = \frac{5}{e^{c \cdot IRI}}$ (C=0,216 for HMA; C=0,286 for PCC); $PSR = 4 - 0,0078 \cdot MRN$ (R²=0,56); $PSR = 4,54 - 20,56 \cdot PI_{Spangler}$ (R² =0,83); $PSR = 6,44 - 0,051 \cdot RQI$; $AI = -1 + \frac{2}{1 + a \cdot e^{(b-cPSR)}}$; PS(%)=100·(1+AI)/2; (Smith et alia, 1997)</p>
3. Present Serviceability Index, PSI	<p>$PSI = 5 - \frac{IRI}{100}$; $PSI = 4,9879 - 0,0078 \cdot IRI$; $PSI = \frac{5}{e^{IRI/5,5}}$; $PSI = 5,26 - 0,0124 \cdot MRN$ (R²=0,91); $PSI = -0,003 \cdot PI + 4,06$ (R²=0,87); $PSI = -0,03881 \cdot PI + 4,629$ (R²=0,74) (PCC); $PSI = -0,04762 \cdot PI + 4,443$ (R²=0,71) (HMA); $PSI = 4,06 - 0,0256 \cdot PI$ (R²=0,87);</p>

	$PSI = 5,41 - 1,80 \cdot \log(1 + SV)$ (PCC); $PSI = 5,03 - 1,91 \cdot \log(1 + SV)$ (HMA); $PSI = 4,66 \cdot e^{0,0065 \cdot QI_r}$ ($R^2=0,83$); $PSI = 4,73 - 0,18 \cdot MO$ ($R^2=0,97$); $PSI = \frac{RCI}{2}$; $PSI = 5 - 0,2937 \cdot [\log(1 + SV)]^4 + 1,1771 \cdot [\log(1 + SV)]^3 - 1,4045 \cdot [\log(1 + SV)]^2 - 1,5803 \cdot [\log(1 + SV)]$; $PSI = 5 + 0,6046 \cdot [\log(1 + SV)]^3 - 2,2217 \cdot [\log(1 + SV)]^2 - 0,0434 \cdot [\log(1 + SV)]$; $PSI = 5 \cdot e^{-0,26 \cdot IRI}$; $PSI = 5 \cdot e^{-0,0041 \cdot IRI}$; (Smith et alia, 1997); www.vti.se/info/rapporter/edetalj.asp
4. Riding Comfort Index, RCI	$RCI = 2 \cdot PSI$; $RCI = 10 \cdot e^{-0,295 \cdot IRI}$; $RCI = 10 \cdot e^{-0,18 \cdot IRI}$; $RCI = 10 \cdot e^{-0,26 \cdot IRI}$; $RCI = 5,4 + 0,02 \cdot crackspacing - \frac{11,6}{(crackspacing)^2}$ (Smith et alia, 1997); http://www.wsdot.wa.gov/ppsc/research/TRBSpecial/TRB2003-000311.pdf
5. Riding Comfort Rating, RCR	$RCR_{car\ users} = 9,11 - 1,39 \cdot IRI$; $RCR_{truck\ users} = 9,37 - 1,71 \cdot IRI$
6. Pavement Quality Index, PQI	$PQI = \sqrt{PSR \cdot SR}$ http://www.ence.umd.edu/~schwartz/courses/ence442/flexible_design_AASHTO.pdf .
7. Ride Number, RN	$RN = 7,86 - 2,35 \cdot \log(MRN)$ (HMA); $RN = 8,66 - 2,704 \cdot \log(MRN)$ (HMA); $RN = 5 \cdot e^{-11,72 \cdot PI^{0,89}}$; $RN = -1,47 - 2,85 \cdot \log(PI)$; $RN = 5 \cdot e^{-160 \cdot PI}$ (Smith et alia, 1997); http://utca.eng.ua.edu/projects/final_reports/99247report.htm ; www.umtri.umich.edu/erd/roughness/iri.html
8. Slope Variance, SV	$SV = 2,2704 \cdot IRI^2$ (Smith et alia, 1997)
9. Mays Ride Number, MRN	$MRN = 43,3 + 5,7 \cdot PI$ ($R^2=0,95$); $MRN = 0,44996 + 0,74515 \cdot IRI$ if $MRN \leq 87,7$; $MRN = -4,42259 + 1,12847 \cdot IRI$ if $MRN > 87,7$ (Smith et alia, 1997)
10. Profile Index, PI	$PI = -22,3 + 0,3 \cdot IRI$ ($R^2=0,92$); $PI = 0,44 \cdot MRN - 20,3$ ($R^2=0,94$); $PI = 0,466 \cdot MRN - 41,4$ ($R^2=0,77$); $PI = 0,168 \cdot MRN - 5,8$ ($R^2=0,57$) (Smith et alia, 1997)
11. Ride Quality Index RQI	$RQI = 35,57 + 675,2 \cdot PI_{Janoff}$ (Smith et alia, 1997)
12. Mays Meter Output, MO	$MO = -25,5 + 0,661 \cdot MRN$ ($R^2=0,87$); $MO = 25,94 + 2,08 \cdot PI - 0,00503 \cdot PI^2$ ($R^2=0,95$); $MO = 18,92 + 0,91524 \cdot ARS$; $MO = 42 \cdot IRI$ (Smith et alia, 1997)
13. RMSVA	$RMSVA = A + \sum B_i \cdot E_{di}$ (Wei and Fwa, 2004)
14. MAVA	$MAVA = A + \sum B_i \cdot E_{di}$ (Wei and Fwa, 2004)
15. SV	$SV = A + \sum B_i \cdot E_{di}$ (Wei and Fwa, 2004)

Table 9 Roughness time-dependence

Indicator	Re-ferences	Relations
1. IRI	$IRI(t) = IRI_0 + 0,081 \cdot t^2 + 2,351 \cdot t$; $\Delta IRI = 134 \exp(m \cdot t) YE4 (1 + SNK)^{-5} + 0,114 \Delta RDS + 0,0066 \Delta ACRX + 0,42 \Delta APOT + m IRI$ $\Delta IRI = \frac{134 \exp(m \cdot AGE3) YE4}{(1 + SNK)^5} + 0,114 \Delta RDS + 0,0066 \Delta ACRX + 0,42 \Delta APOT + m IRI_a$; $IRI_{MIN} = MAX\{1, MIN[7,7, 0,36 D95(1 - 2,78 MGD)]\}$; $IRI_{MAX} = MAX[11,5, 21,5 - 32,4(0,5 - MGD)^2 + 0,017 CV - 0,76 RF MMP]$ $IRI_{AV} = \frac{IRI_{MAX} + (0,447 - 0,230 MGD)(1 - \exp(C \cdot BLFQ))(IRI_{MAX} - IRI_{MIN})}{(1 - (0,553 + 0,230 MGD) \exp(C \cdot BLFQ)) C \cdot BLFQ}$ $C = -0,001(0,461 + 0,0174 ADL + 0,0114 ADH - 0,0287 ADT MMP)$ $dIRI = 0,016 + 0,0524 \cdot IRI(t)$; $dIRI = 0,036 + 0,0560 \cdot IRI(t)$; $dIRI = 0,016 + 0,0524 \cdot IRI(t)$; $dIRI = 0,036 + 0,0560 \cdot IRI(t)$ (Smith et alia, 1997); (Tammirinne, 2002)	
2. PSR	$PSR(t) = 5 - 0,24 \cdot t$	

	(Smith et alia, 1997)
3. PSI	$PSI(t) = 5 - 0,2 \cdot t$ (Smith et alia, 1997)
4. PCI	$PCI(t) = 100 - 3,5 \cdot t$ (Smith et alia, 1997)
5. PCR	$PCR = 100 - \beta_1 t^{\beta_2}$; PCC: $PCR = 96.0 - 3.7(AGE)$; $PCR = 96.2 - 7.0 (AGE)$; $PCR = 99.1 - 0.9 (AGE)$; HMA: $PCR = 98.1 - 3.3 (AGE)$; $PCR = 98.6 - 3.8 (AGE)$; $PCR = 98.3 - 3.3 (AGE)$; $PCR = 98.0 - 3.3 (AGE)$; $PCR = 98.0 - 3.4 (AGE)$; $PCR = 99.5 - 2.0 (AGE)$; composite pavements: $PCR = 96.1 - 3.0 (AGE)$; $PCR = 96.1 - 3.8 (AGE)$ $PCR = 96.1 - 3.3 (AGE)$; $PCR = 96.1 - 3.3 (AGE)$; $PCR = 96.0 - 3.7 (AGE)$; $PCR = 99.6 - 3.3 (AGE)$; [http://www.dot.state.oh.us/pavement/Pubs/Sect100.pdf Pavement Deterioration Models]
6. RN	$RN(Y_2) = (RN(Y_1)e^{(0.0153(t_2-t_1))}) + (5.7(1+SNC)(-4.99)EDA(t_2-t_1))e^{(0.0153t_2)}$; (Patrick, 2003)
7. RCI	$RCI_t = \beta_0 + \beta_1 \cdot \ln(RCI_0) + \beta_2 \cdot \ln(t^2 + 1) + \beta_3 \cdot t + \beta_4 \cdot t \cdot \ln(RCI_0) + \beta_5 \cdot \Delta t$
8. RDM	$RDM = K_{rp} \frac{39800(YE4 \cdot 10^6)^{ERM}}{SNC^{0.502} COMP^{2.30}}$; $\Delta RDM = K_{rp} RDM \left(\frac{0.166 + ERM}{AGE^3} + 0.0219 MMP \Delta CRX \ln(\max(1, AGE^3 YE4)) \right)$ where: $ERM = 0.09 - 0.0009 RH + 0.0384 DEF + 0.00158 MMP CRX$; $K_{rp} = \frac{GeomAverage[ORDM_j]}{GeomAverage[PRDM_j]}$ or $K_{rp} = \frac{SUM[\log(ORDM_j)]}{SUM[\log(PRDM_j)]}$
9. Ruts, RDS	$RDS = K_{rp} \frac{4390 \Delta RDM^{0.532} (YE4 \cdot 10^6)^{ERS}}{SNC^{0.422} COMP^{1.66}}$; $\Delta RDS = K_{rp} RDS \left(\frac{0.532 + \Delta RDM}{RDM} + \frac{ERS}{AGE^3} + 0.0519 MMP \Delta CRX \ln(\max(1, AGE^3 YE4)) \right)$ where: $ERS = -0.0086 RH + 0.00115 MMP CRX$ $K_{rp} = \frac{Geom. Average[ORDS_j]}{Geom. Average[PRDS_j]}$ or $K_{rp} = \frac{SUM[\log(ORDS_j)]}{SUM[\log(PRDS_j)]}$
10. RI	$RI_t = 0.98 \exp(m AGE3) RI_0 + \frac{135 NE4_t}{(1 + SNK)^5} + 0.143 RDS_t + 0.0068 ACRX_t + 0.056 APAT_t$ $RI_t = 1.04 \exp(m AGE3) \left[RI_0 + \frac{263 NE4_t}{(1 + SNK)^5} \right]$; $RI_a = RI_b + \max\{0, \max[0.3(5.4 - RI_b), 0.5]\} - 0.0066 ACX$ $RI_a = 3.85 - \frac{\min(H, 80) + \min(H, 40)}{52} + \frac{28 \max(RI_b - 3.85)}{\max(H, 28)}$